HHS Public Access

Author manuscript

Clin Sci (Lond). Author manuscript; available in PMC 2021 May 17.

Published in final edited form as:

Clin Sci (Lond). 2018 November 15; 132(21): 2357–2368. doi:10.1042/CS20180749.

Prevention of perinatal nicotine-induced bone marrow mesenchymal stem cell myofibroblast differentiation by augmenting the lipofibroblast phenotype

Reiko Sakurai, **Jie Liu**, **Ying Wang**, **John S. Torday**, **Virender K. Rehan**

Department of Pediatrics, Los Angeles Biomedical Research Institute at Harbor-UCLA Medical Center, Torrance, CA, USA

Abstract

Perinatal nicotine exposure drives the differentiation of alveolar lipofibroblasts (LIFs), which are critical for lung injury repair, to myofibroblasts (MYFs), which are the hallmark of chronic lung disease. Bone marrow-derived mesenchymal stem cells (BMSCs) are important players in lung injury repair; however, how these cells are affected with perinatal nicotine exposure and whether these can be preferentially driven to a lipofibroblastic phenotype are not known. We hypothesized that perinatal nicotine exposure would block offspring BMSCs lipogenic differentiation, driving these cells toward a MYF phenotype. Since peroxisome proliferator activated-receptor γ (PPARγ) agonists can prevent nicotine-induced MYF differentiation of LIFs, we further hypothesized that the modulation of PPARγ expression would inhibit nicotine's myogenic effect on BMSCs. Sprague Dawley dams were perinatally administered nicotine (1 mg/kg bodyweight) with or without the potent PPARγ agonist rosiglitazone (RGZ), both administered subcutaneously. At postnatal day 21, BMSCs were isolated and characterized morphologically, molecularly, and functionally for their lipogenic and myogenic potentials. Perinatal nicotine exposure resulted in decreased oil red O staining, triolein uptake, expression of PPARγ, and its downstream target gene adipocyte differentiation-related protein by BMSCs, but enhanced α-smooth muscle actin and fibronectin expression, and activated Wnt signaling, all features indicative of their inhibited lipogenic, but enhanced myogenic potential. Importantly, concomitant treatment with RGZ virtually blocked all of these nicotine-induced morphologic, molecular, and functional changes. Based on these data, we conclude that BMSCs can be directionally induced to differentiate into the lipofibroblastic phenotype, and PPARγ agonists can effectively block perinatal nicotine-induced MYF transdifferentiation, suggesting a possible molecular therapeutic approach to augment BMSC's lung injury/repair potential.

Correspondence: Virender K. Rehan (vrehan@labiomed.org).

Author Contribution

V.K.R. conceived and designed the experiments. R.S., J.L., and Y.W. performed the experiments. R.S., J.L., Y.W., and V.K.R. analyzed the data. R.S., J.S.T., and V.K.R. wrote the paper.

Competing Interests

The authors declare that there are no competing interests associated with the manuscript.

Introduction

Despite the well-publicized risks, more than 10% of U.S. women smoke during pregnancy, resulting in at least 400,000 smoke-exposed infants/year [1]. The direct effects of maternal smoking on the developing fetus have been attributed mainly to nicotine, which crosses the human placenta with minimal biotransformation, and accumulates in fetal blood and amniotic fluid despite increased nicotine clearance during pregnancy, resulting in even higher fetal plasma and tissue levels than those in the smoking mother [2,3]. Furthermore, the recent exponential increase in the use of electronic cigarettes and the frequent use of the nicotine patch as a nicotine replacement strategy in pregnant smokers render comprehensive investigation on the consequences of nicotine exposure on the developing fetus [4–6].

Alveolar lipofibroblasts (LIFs) are critical for lung homeostasis and injury/repair [7,8]. Our laboratory has previously shown that both *in vitro* and *in utero* nicotine exposures drive the differentiation of LIFs to myofibroblasts (MYFs), a cell-type that is not conducive to alveolar homeostasis, and is the ‘hallmark’ of chronic lung disease [9,10]. Lung injury stimulates the recruitment of bone marrow-derived mesenchymal stem cells (BMSCs) for repair [11–13], whereas the environment these cells are in, both systemically and locally [14], is critical for their healing effects. It has been shown that under appropriate conditions, BMSCs can differentiate into a wide variety of cell-types, and that they play a critical role in lung injury/repair. However, how the lipogenic potential of perinatal nicotine-exposed BMSCs is affected is unknown. Furthermore, whether a targeted intervention, e.g. parenteral administration of a peroxisome proliferator-activated receptor γ (PPARγ) agonist, augments the lipogenic potential of BMSCs is also unknown. We hypothesized that perinatal nicotine exposure drives BMSCs toward a myogenic phenotype, blocking their lipogenic potential, and that a simultaneous PPARγ agonist administration would drive these cells to a lipofibroblastic phenotype, preventing nicotine-induced myogenic phenotype. Therefore, here we determine how perinatal nicotine exposure affects rat offspring BMSC differentiation, and whether the PPARγ agonist rosiglitazone (RGZ) could prevent nicotine-induced BMSC myogenic differentiation.

Materials and methods

Animals

In line with our previous work, time-mated first time pregnant Sprague Dawley rat dams (200–250 g body weight) were administered either diluent (saline), nicotine (1 mg/kg) or nicotine + rosiglitazone (RGZ, 3 mg/kg) subcutaneously once a day in 100 μl volumes from the sixth day of gestation until term (= day 22) to postnatal day 21 [9,13]. The dose of nicotine used in this study is approximately equivalent to that of a moderately heavy smoker, i.e. ~1 mg/kg body weight/day [15–17] and the dose of RGZ used has been previously demonstrated to block the perinatal nicotine-induced lung phenotype in the rat model used in this study [18]. The control and nicotine-treated dams were pair-fed with free access to water, and were maintained in a 12 h:12 hlight:dark cycle. After spontaneous delivery at term, the pups were allowed to breast feed ad libitum and at postnatal day (PND) 21, the rats were killed, and the BMSCs were isolated and maintained in culture, as outlined below, following the previously described methods [19–21]. All animal procedures were performed

following the guidelines of the National Institutes of Health for the care and use of laboratory animals after approval of the Los Angeles Biomedical Research Institute Animal Care and Use Committee.

Isolation of bone marrow-derived mesenchymal stem cells

The medullary cavities of rat femurs were flushed with Minimal Essential Medium (MEM) Alpha (1×) + GlutaMax™-1 (Cat No.: 32561–037, Life Technologies) containing 1% penicillin-streptomycin (anti-anti). The cells were washed once with MEM and plated at 1×10^6 cells per T75 flask (Corning, Corning, NY) in the complete medium: MEM Alpha containing 10% fetal bovine serum (FBS) and 1% anti-anti (Gibco, Life Technologies, Grand Island, NY, catalog# 15240–062), and cultured at 37°C in 5% CO_2. Non-adherent cells were removed and fresh media was added every 48 h. At confluence, the cells were harvested and using magnetic beads (Miltenyi Biotech, Auburn, CA), macrophages were depleted with anti-CD11b antibody, and other hematopoietic cells were removed using an anti-CD45 (both from BD Biosciences, Palo Alto, CA). Cells were collected in 1 ml of DMEM supplemented with 10% FBS, and then cultured and passaged. Due to >95% purity of cells at passage (P) 3, all experiments were conducted at P3.

Flow cytometry

For flow cytometry, the adherent cells were removed by trypsinization, washed with Ca^{2+}, Mg^{2+}-containing 1× phosphate buffered saline (PBS) and blocked with 3% fetal bovine serum (FBS) in PBS for 30 min at 4°C. Cells were aliquoted (100 µl/tube) for binding and staining with 2.5 µg/ml of FITC- or Alexa Fluor (AF)-conjugated antibodies. Sorting was performed using a BD Biosciences fluorescence-activated cell sorting (FACS) DiVa High-Speed Cell Sorter (San Diego, CA) with 350, 488, and 633 nm lasers. Anti-CD34 to Alexa Fluor 488 and anti-Stro-1 were conjugated to Alexa Fluor 488, anti-CD45 to FITC, anti-CD90 to PE, anti-CD105 to Alexa Fluor 488, and to the appropriate isotype controls (all from BD Pharmingen Inc., San Diego, CA except anti-Stro-1, which was obtained from Invitrogen, Carlsbad, CA). The data were analyzed using FlowJo software (Tree Star, San Carlos, CA). Propidium iodide was used to exclude dead cells, and percentages of positively stained-cells were calculated by subtracting the value of isotype controls. Cells were negatively selected for CD34 (NOVUS, catalog# NB600–107 AF 488) and CD45 (BD Pharmingen, Catalog# 554877 FITC) and positively selected for CD90 (BD Pharmingen Catalog# 554898 PE), CD105 (Application.Inc, catalog# CA1725), and Stro-1 (Invitrogen, catalog# 398407).

Multipotent potential of cells

Multipotent potential of cells was confirmed by determining their adipogenic, myogenic, and osteogenic potentials, as outlined below.

Adipogenic induction

For adipogenic induction, cells cultured in six-well plates were treated with adipogenic induction medium (MEM + 10% FBS, supplemented with 10 µM dexamethasone, 0.5 mM 3-isobutyl-1-methylxanthine, 10 µg/ml insulin, and 50 µM indomethacin), which was

changed every 2 days for a total of 6 days, following which oil Red O (ORO) staining was performed. Briefly, cells were fixed in 4% paraformaldehyde for 15 min and washed with 1× PBS. About 300 μl of ORO was added to the slides and kept for 30 min at room temperature. The slides were washed with $ddH_2O \times 3$ and mounted with DAPI-mounting medium from Vector Laboratories. Inc.

Myogenic induction

For myogenic induction, cells were treated with transforming growth factor-β (10 ng/ml), insulin (1 μg/ml), transferrin (0.55 μg/ml), and selenium (670 ng/ml), all from Invitrogen, Carlsbad, CA, for 72 h, following which cells were immunostained for α-smooth muscle actin (α-SMA).

Osteogenic induction

Osteogenic differentiation was accomplished by culturing cells in MEM, supplemented with 5% FBS, 100 nM dexamethasone, 10 mM b-glycerophosphate, and 50 μg/ml ascorbic acid for 10–14 days, following which cells were fixed with formalin and stained for calcium phosphate with alizarin red S.

RNA isolation and quantitative real-time PCR

Total RNA was isolated from cultured BMSCs using Qiagen RNAeasy plus mini kit (Qiagen Applied Biosystems, Foster City, CA, Cat. No.: 74134); the extracted RNA was quantitated by absorbance using a nanodrop spectrophotometer (Nanodrop Instruments, Wilmington, DE), and processed for q-RT-PCR according to our previously described method [19]. All PCR primers were obtained from Sigma-Aldrich (St. Louis, MO), which included 18S: 5′-GGACAGGATTGACAGATTGATAGC-3′ (forward) and 5′-GGTTATCGGAATTAACCAGACAA-3′ (reverse); adipocyte differentiation-related protein (ADRP): 5′-ATTCTGGACCGTGCCGATT-3′ (forward) and 5′-CTGCTACTGATGCCATTTTTCCT-3′ (reverse); PPARγ: 5′-CCAAGTGACTCTGCTCAAGTATGG-3′ (forward) and 5′-CATGAATCCTTGTCCCTCTGATATG-3′ (reverse); α-SMA: 5′-GAGAAGAGTTACGAGTTGCCTGATG-3′ (forward) and 5′-CACGCGAAGCTCGTTATAGAAG-3′ (reverse); fibronectin: 5′-GTGCCTGGGGACCTCGGTGCGC-3′ (forward), and 5′-TGTCAAAACAGCCAGGCTTGC-3′(reverse). All RT-qPCRs were performed in triplicate on an ABI StepOnePlus System. The relative mRNA level was calculated using the $2^{-\Delta\Delta C_T}$ method, with β-actin mRNA as a normalizer.

Western blot analysis

Protein extraction and Western blot analyses for PPARγ, ADRP, α-SMA, and fibronectin were performed as previously described [9,10,18]. Briefly, cells were homogenized in 10 mM Tris (pH 7.5), 0.25 M sucrose, 1 mM EDTA, 5 mM benzamidine, 2 mM phenylmethylsulfonyl fluoride, and 10 μg/ml each of pepstatin A, aprotinin, and leupeptin, and centrifuged at 14000 rpm for 10 min at 4°C. Equal amounts of protein from the supernatant were dissolved in electrophoresis sample buffer and subjected to SDS-

polyacrylamide (4–12% gradient) gel electrophoresis, followed by electrophoretic transfer to a nitrocellulose membrane. The membrane was blocked with 5% milk in 1× Tris-buffered saline containing 0.1% Tween 20 for 1 h, and then incubated with primary antibody from Santa Cruz Biotechnology Inc. except α-SMA [PPARγ (1:150, Catalog# sc-7196), ADRP (1:200, Catalog# sc-32888), α-SMA (1:5000, Sigma-Aldrich, Catalog# A2547), and fibronectin (1:3000, Catalog# sc-9086)] overnight at 4°C. Subsequently, the membrane was washed with 1× Tris-buffered saline + 0.1% Tween 20, and incubated with the appropriate secondary antibody for 1 h at room temperature, washed again, and developed with SuperSigal West Pico chemiluminescent substrate (Pierce Biotechnology, Rockford IL) following the manufacturer's protocol. The densities of the PPARγ, ADRP, α-SMA, and fibronectin bands were quantitated using a scanning densitometer UN-SCAN-IT software (Silk Scientific, Orem.UT) and normalized to glyceraldehydephosphate (GAPDH).

Immunocytochemistry

Bone marrow derived mesenchymal stem cells were grown in slide-backed chambers (Lab-Tek; Electron Microscopy Sciences, Hatfield, Pennsylvania). The cells were blocked with 5% normal goat serum and subsequently incubated with primary and secondary antibodies. For α-SMA staining, mouse monoclonal anti-α-SMA antibody (1:800; Sigma-Aldrich.Catalog# A2547) was used as the primary antibody. After several PBS washes at room temperature, the cells were incubated with the appropriate Alexa Fluor secondary antibody (1:800, antimouse Alexa Fluor 488 Green, from Invitrogen) in a humidified, darkened chamber. Slides were gently rinsed with PBS and mounted with ProLong Gold antifade reagent with DAPI (Invitrogen) for fluorescent microscopic analysis.

Triglyceride uptake assay

The rate of [^{3}H]-triolein uptake was assayed as a marker for triglyceride uptake, as described by us previously [22].

Statistical analysis

The data were analyzed, using either ANOVA or student's *t*-test, as appropriate. The results are based on 4–6 independent experiments and the values are expressed as mean ± SD. A P value of ≤0.05 is considered to represent statistically significant difference between the experimental groups.

Results

Stem cell characterization of BMSCs

As described by us recently, control P3 BMSCs isolated and subjected to FACS analysis were negative for CD34 and CD45, >90% positive for CD105, >95% positive for CD90 and Stro-1 [19]. Importantly, nicotine and nicotine + RGZ treatments did not affect the percentage of cells expressing these cell surface markers (Figure 1). Furthermore, using the above described protocols, multipotent potential of the isolated cells was confirmed by their induction to adipocytes (positive ORO staining), myocytes (positive α-SMA staining**)**, and osteocytes (positive Alizarin red S staining). Taken together, these data confirm the non-endothelial BMSC nature of the isolated cells.

Effect of perinatal nicotine exposure on BMSC adipogenic and myogenic potential

The control BMSCs exhibited virtually no ORO staining and very little α-SMA staining at baseline (Figure 2A,C), but after adipogenic and myogenic inductions, there were strongly positive ORO and α-SMA staining, respectively (Figure 2B,D). Compared with controls, perinatal nicotine (1 mg/kg) exposed cells demonstrated decreased lipid, and increased α-SMA staining, upon adipogenic and myogenic inductions, respectively (Figure 2B,D). This effect was blocked by concomitant perinatal treatment with RGZ (3 mg/kg) (Figure 2B,D). Triglyceride uptake, a hallmark of the LIF, was also significantly decreased in perinatal nicotine-exposed BMSCs, an effect that was effectively blocked by simultaneous perinatal RGZ treatment. In fact, RGZ-exposed BMSCs had even higher triolein uptake compared with the untreated controls (Figure 3).

Effect of perinatal nicotine exposure on the determinants of BMSC lipofibroblast versus myofibroblast phenotype

PPARγ, a key nuclear transcription factor that determines the lipofibroblastic phenotype was significantly inhibited in the perinatal nicotine-exposed cells, both at the protein and mRNA levels, with RGZ treatment blocking this effect, also at both the mRNA and protein levels (Figure 4A). A similar effect of perinatal nicotine exposure and RGZ treatment on BMSCs was observed for ADRP, which is a down-stream target of PPARγ, showing down-regulation by perinatal nicotine exposure, and its blockage by perinatal RGZ treatment (Figure 4B). Expression of the myogenic markers α-SMA and fibronectin was significantly increased by perinatal nicotine exposure, an effect that was completely blocked by perinatal RGZ treatment (Figure 5A,B).

Effect of perinatal nicotine exposure on BMSC Wnt signaling

Having determined the suppression of PPARγ signaling and activation of myogenic markers in BMSCs following perinatal nicotine exposure, we next determined the expression of Wnt signaling, the key determinant of the myofibroblastic phenotype. A Wnt-specific array (SABiosciences, Frederick, MD, U.S.A.) was performed, which provides information for 84 specific genes involved in Wnt signaling. As shown in Figure 6, 15 genes, belonging to the canonical Wnt pathway (Axin2, Wnt6, Dkk1, Sfrp2, Tcf7, APC2, and Csnk1a1), the non-canonical Wnt/calcium pathway (Frzb, Wnt5b, and Wnt11), negative regulators of Wnt receptor signaling (Axin2, Ccnd1, Dkk1, Tie1, and Srfp2), and other Wnt signaling pathway-related genes (Bcl9 and Fzd7) showed >2-fold change, with 14 of these genes up-regulated and one gene down-regulated. These genes regulate various developmental processes including but not limited to cell cycle regulation, cell migration, and cellular homeostasis. Remarkably, 10 of the 14 up-regulated genes and the only down-regulated gened were normalized in the RGZ-treated group.

Discussion

Based on the observations made in this series of experiments, perinatal nicotine exposure inhibits rat offspring BMSC lipogenic potential, but enhances their myogenic potential. The potent PPARγ agonist RGZ effectively blocks the nicotine-induced BMSC transdifferentiation to a myogenic phenotype, offering a potentially therapeutic intervention.

Lipofibroblasts, the lung alveolar adepithelial adipocyte-like cells, are critical for lung injury/repair since they actively provide triglyceride substrate to alveolar epithelial type II cells for surfactant synthesis [23,24], support alveolar type II cell growth and differentiation [25], and act as an important defense against oxidant lung injury [26]. Though the progenitors of LIFs and the process of induction and differentiation of LIFs are incompletely understood, in general adipogenesis is known to occur in two major phases: the 'determination' phase and the 'terminal differentiation' phase. In the 'determination' phase, multipotent BMSCs become committed to the adipocyte lineage, and lose their ability to differentiate into other mesenchymal lineages. In this phase, committed preadipoctytes are morphologically indistinguishable from their precursors. During the 'terminal differentiation' phase, fibroblastic preadipocytes are converted to spherical, mature adipocytes that can synthesize and transport lipids, secrete adipocyte-specific proteins, and express the machinery necessary for insulin sensitivity. From the data included here and our previously published work [27,28], nicotine seems to affect both the 'determination' and 'terminal differentiation' phases of adipogenesis.

Adipogenesis reflects a fundamental shift in gene expression pattern within uncommitted BMSCs that promote and culminate in the phenotypic properties that define mature adipocytes. Adipogenesis is driven by a complex, well-orchestrated signaling cascade involving regulated changes in the expression and/or activity of several key transcription factors, most notably PPARγ and CCAAT enhancer binding protein α. BMSC adipogenesis is characterized by a dramatic increase in PPARγ expression [29], which activates or induces the expression of the majority of genes that characterize the adipocytic phenotype, including ADRP. Given our data, it is clear that perinatal nicotine exposure shifts the BMSC differentiation potential from adipogenic to myogenic, possibly providing at least one of the mechanisms for the increased predisposition to chronic lung disease following perinatal smoke/nicotine exposure. However, PPARγ agonist treatment not only blocked this adipogenic-to-myogenic shift, but also promoted BMSC differentiation to an adipogenic phenotype, as has been demonstrated previously [30].

Alveolar interstitial lung LIFs were first discovered in the lungs of fetal and adult rats in 1970 [31]. The structural and biochemical characteristics of this cell-type were detailed in the late 1970s and early 1980s [32–34]. Based on their lipid-containing phenotype, the pulmonary interstitial cell population was divided into two populations—those with and without lipid droplets [32]. Subsequently, the lipid-containing fibroblasts were determined to be Thy-1 positive [35]. A population of lung interstitial fibroblasts that are both Thy-1 (or CD90) and Sca-positive has been identified [36], indicating that some LIFs are lung stem cells. Though the origins of these cells still need to be determined, the current data demonstrating that the BMSCs are CD90 positive and can differentiate into adipocytes, suggest that the bone marrow can contribute to this pool of cells. Seen in the light of our extensive experimental evidence that the LIF acts to both promote alveolar homeostasis and protect the alveolus against injury [4,7,8], we speculate that this mechanism is due, in part, to the recruitment of BMSCs.

Using a biologic model of lung development, homeostasis and repair [4,7,8], we have previously determined that *in utero* nicotine exposure disrupts specific alveolar molecular

paracrine communications between the epithelium and interstitium, resulting in the transdifferentiation of lung LIFs to MYFs, i.e., the conversion of the LIF phenotype to a cell-type that is not conducive to alveolar homeostasis, and that is the cellular hallmark of chronic lung disease, including asthma [4,8,9,25]. Furthermore, we have shown that by molecularly targeting PPARγ expression, nicotine-induced lung injury can not only be significantly averted, but also possibly be reverted [37,38]. The therapeutic implications of these observations should be considered in light of the current finding that nicotine also inhibits BMSC adipogenic differentiation. Therefore, nicotine may not only affect the resident lung fibroblasts in the developing lung tissue, but also affect the BMSCs, recruited from bone marrow for lung development and injury repair. Our findings for first time suggest that nicotine has a global detrimental effect on mesenchymal cell differentiation during lung development and injury repair. Therefore, instead of administering BMSCs [39], systemic administration of a PPARγ agonist, which can potentially stimulate both alveolar epithelial–mesenchymal and BMSC paracrine interactions [4,7,8] and promote BMSCs' adipogenic phenotype [30,40], may be a more effective approach to rescue and reverse the adverse effects of perinatal nicotine exposure. However, it is important to acknowledge that the effects of PPARγ agonists' administration on the developing offspring's BMSCs in the absence of nicotine/smoke exposure remain to be studied, an important limitation of the present study.

Based on the observations made in this series of experiments, BMSCs can be directed to differentiate into the LIF phenotype. Treatment with a PPARγ agonist can enhance BMSC LIF induction. Perinatal nicotine exposure inhibits offspring BMSCs lipogenic differentiation, but enhances their myogenic differentiation. The fact that a potent PPARγ agonist can effectively block nicotine-induced BMSC transdifferentiation to the MYF phenotype offers a potential therapeutic approach, which has been also shown to be effective in other models of lung injury repair.

Acknowledgments

Funding

This work was supported by [HL127137, HD071731] from the NIH; and [23RT-0018 and 27IP-0050] from the TRDRP.

Abbreviations

α-SMA	α-smooth muscle actin
ADRP	adipocyte differentiation-related protein
BMSC	bone marrow-derived mesenchymal stem cell
FBS	fetal bovine serum
LIF	lipofibroblast
MEM	minimum essential medium
MYF	myofibroblast

ORO	oil red O
PND	postnatal day
PPARγ	peroxisome proliferator activated-receptor γ
RGZ	rosiglitazone maleate

References

1. Tong VT, Dietz PM, Morrow B, D'Angelo DV, Farr SL, Rockhill KM et al. (2013) Trends in smoking before, during, and after pregnancy–Pregnancy Risk Assessment Monitoring System, United States, 40 sites, 2000–2010. Morbidity And Mortality Weekly Report Surveillance Summaries (Washington, DC: 2002) 62, 1–19
2. Dempsey D, Jacob P III, Benowitz NL (2002) Accelerated metabolism of nicotine and cotinine in pregnant smokers. J. Pharmacol. Exp. Therapeutics 301, 594–598, 10.1124/jpet.301.2.594
3. Matta SG., Balfour DJ., Benowitz NL., Boyd RT., Buccafusco JJ., Caggiula AR. et al.. (2007) Guidelines on nicotine dose selection for in vivo research. Psychopharmacology 190, 269–319, 10.1007/s00213-006-0441-0 [PubMed: 16896961]
4. Rehan VK, Asotra K and Torday JS (2009) The effects of smoking on the developing lung: insights from a biologic model for lung development, homeostasis, and repair. Lung 187, 281–289, 10.1007/s00408-009-9158-2 [PubMed: 19641967]
5. Weaver SR, Kemp CB, Heath JW, Pechacek TF and Eriksen MP (2017) Use of Nicotine in Electronic Nicotine and Non-Nicotine Delivery Systems by US Adults, 2015. Public Health Reports (Washington, DC: 1974) 132, 545–548, 10.1177/0033354917723597
6. Yoong SL, Stockings E, Chai LK, Tzelepis F, Wiggers J, Oldmeadow C et al. (2018) Prevalence of electronic nicotine delivery systems (ENDS) use among youth globally: a systematic review and meta-analysis of country level data. Aust. N. Z. J. Public Health 42, 303–308, 10.1111/1753-6405.12777 [PubMed: 29528527]
7. Rehan VK. and Torday JS. (2014) The lung alveolar lipofibroblast: an evolutionary strategy against neonatal hyperoxic lung injury. Antioxid. Redox Signal 21, 1893–1904, 10.1089/ars.2013.5793 [PubMed: 24386954]
8. Torday JS and Rehan VK (2007) Developmental cell/molecular biologic approach to the etiology and treatment of bronchopulmonary dysplasia. Pediatr. Res 62, 2–7, 10.1203/PDR.0b013e31806772a1 [PubMed: 17515838]
9. Krebs M, Sakurai R, Torday JS and Rehan VK (2010) Evidence for in vivo nicotine-induced alveolar interstitial fibroblast-to-myofibroblast transdifferentiation. Exp. Lung Res 36, 390–398, 10.3109/01902141003714023 [PubMed: 20715982]
10. Rehan VK, Wang Y, Sugano S, Romero S, Chen X, Santos J et al. (2005) Mechanism of nicotine-induced pulmonary fibroblast transdifferentiation. Am. J. Physiol. Lung Cell. Mol. Physiol 289, L667–L676, 10.1152/ajplung.00358.2004 [PubMed: 15951329]
11. Frenette PS, Pinho S, Lucas D and Scheiermann C (2013) Mesenchymal stem cell: keystone of the hematopoietic stem cell niche and a stepping-stone for regenerative medicine. Annu. Rev. Immunol 31, 285–316, 10.1146/annurev-immunol-032712-095919 [PubMed: 23298209]
12. Ortiz LA, Gambelli F, McBride C, Gaupp D, Baddoo M, Kaminski N et al. (2003) Mesenchymal stem cell engraftment in lung is enhanced in response to bleomycin exposure and ameliorates its fibrotic effects. Proc. Natl. Acad. Sci. U.S.A 100, 8407–8411, 10.1073/pnas.1432929100 [PubMed: 12815096]
13. Rojas M, Xu J, Woods CR, Mora AL, Spears W, Roman J et al. (2005) Bone marrow-derived mesenchymal stem cells in repair of the injured lung. Am. J. Respir. Cell Mol. Biol 33, 145–152, 10.1165/rcmb.2004-0330OC [PubMed: 15891110]
14. Fung ME and Thebaud B (2014) Stem cell-based therapy for neonatal lung disease: it is in the juice. Pediatr. Res 75, 2–7, 10.1038/pr.2013.176 [PubMed: 24126817]

15. Benowitz NL. (1988) Drug therapy. Pharmacologic aspects of cigarette smoking and nicotine addiction. New Eng. J. Med 319, 1318–1330, 10.1056/NEJM198811173192005 [PubMed: 3054551]

16. Eskenazi B and Bergmann JJ (1995) Passive and active maternal smoking during pregnancy, as measured by serum cotinine, and postnatal smoke exposure. I. Effects on physical growth at age 5 years. Am. J. Epidemiol 142, S10–S18, [PubMed: 7572982]

17. Holloway AC, Kellenberger LD and Petrik JJ (2006) Fetal and neonatal exposure to nicotine disrupts ovarian function and fertility in adult female rats. Endocrine 30, 213–216, 10.1385/ENDO:30:2:213 [PubMed: 17322582]

18. Liu J, Sakurai R, O'Roark EM, Kenyon NJ, Torday JS and Rehan VK (2011) PPARgamma agonist rosiglitazone prevents perinatal nicotine exposure-induced asthma in rat offspring. Am. J. Physiol. Lung Cell. Mol. Physiol 300, L710–L717, 10.1152/ajplung.00337.2010 [PubMed: 21355041]

19. Gong M., Antony S., Sakurai R., Liu J., Iacovino M. and Rehan VK. (2016) Bone marrow mesenchymal stem cells of the intrauterine growth-restricted rat offspring exhibit enhanced adipogenic phenotype. Int. J.Obesity 40, 1768–1775, 10.1038/ijo.2016.157

20. Miranda SC, Silva GA, Hell RC, Martins MD, Alves JB and Goes AM (2011) Three-dimensional culture of rat BMMSCs in a porous chitosan-gelatin scaffold: A promising association for bone tissue engineering in oral reconstruction. Arch. Oral. Biol 56, 1–15, 10.1016/j.archoralbio.2010.08.018 [PubMed: 20887975]

21. Tseng FW, Tsai MJ, Yu LY, Fu YS, Huang WC and Cheng H (2013) Comparative effects of bone marrow mesenchymal stem cells on lipopolysaccharide-induced microglial activation. Oxidative Med. Cell. Longev 2013, 234179, 10.1155/2013/234179

22. Karadag A, Sakurai R, Wang Y, Guo P, Desai M, Ross MG et al. (2009) Effect of maternal food restriction on fetal rat lung lipid differentiation program. Pediatr. Pulmonol 44, 635–644, 10.1002/ppul.21030 [PubMed: 19514059]

23. Torday J, Hua J and Slavin R (1995) Metabolism and fate of neutral lipids of fetal lung fibroblast origin. Biochim. Biophys. Acta 1254, 198–206, 10.1016/0005-2760(94)00184-Z [PubMed: 7827125]

24. Torday J and Rehan V (2011) Neutral lipid trafficking regulates alveolar type II cell surfactant phospholipid and surfactant protein expression. Exp. Lung Res 37, 376–386, 10.3109/01902148.2011.580903 [PubMed: 21721951]

25. Torday JS., Torres E. and Rehan VK. (2003) The role of fibroblast transdifferentiation in lung epithelial cell proliferation, differentiation, and repair in vitro. Pediatr. Pathol. Mol. Med 22, 189–207, 10.1080/pdp.22.3.189.207 [PubMed: 12746170]

26. Torday JS, Torday DP, Gutnick J, Qin J and Rehan V (2001) Biologic role of fetal lung fibroblast triglycerides as antioxidants. Pediatr. Res 49, 843–849, 10.1203/00006450-200106000-00021 [PubMed: 11385147]

27. Rehan VK and Torday JS (2012) PPARgamma signaling mediates the evolution, development, homeostasis, and repair of the lung. PPAR Res. 2012, 289867, 10.1155/2012/289867 [PubMed: 22792087]

28. Sakurai R, Cerny LM, Torday JS and Rehan VK (2011) Mechanism for nicotine-induced up-regulation of Wnt signaling in human alveolar interstitial fibroblasts. Exp. Lung Res. 37, 144–154, 10.3109/01902148.2010.490288 [PubMed: 21133803]

29. Ylostalo J, Smith JR, Pochampally RR, Matz R, Sekiya I, Larson BL et al. (2006) Use of differentiating adult stem cells (marrow stromal cells) to identify new downstream target genes for transcription factors. Stem Cells 24, 642–652, 10.1634/stemcells.2005-0270 [PubMed: 16439615]

30. Benvenuti S, Cellai I, Luciani P, Deledda C, Baglioni S, Giuliani C et al. (2007) Rosiglitazone stimulates adipogenesis and decreases osteoblastogenesis in human mesenchymal stem cells. J. Endocrinol. Invest 30, Rc26–Rc30, 10.1007/BF03350807 [PubMed: 17993761]

31. O'Hare KH and Sheridan MN (1970) Electron microscopic observations on the morphogenesis of the albino rat lung, with special reference to pulmonary epithelial cells. Am. J. Anat 127, 181–205, 10.1002/aja.1001270205 [PubMed: 5413181]

32. Brody JS and Kaplan NB (1983) Proliferation of alveolar interstitial cells during postnatal lung growth. Evidence for two distinct populations of pulmonary fibroblasts. Am. Rev. Respir. Dis 127, 763–770 [PubMed: 6859658]

33. Brody JS and Vaccaro C (1979) Postnatal formation of alveoli: interstitial events and physiologic consequences. Fed. Proc 38, 215–223 [PubMed: 761655]

34. Vaccaro C and Brody JS (1978) Ultrastructure of developing alveoli. I. The role of the interstitial fibroblast. Anat. Rec 192, 467–479, 10.1002/ar.1091920402 [PubMed: 736269]

35. Phipps RP, Penney DP, Keng P, Quill H, Paxhia A, Derdak S et al. (1989) Characterization of two major populations of lung fibroblasts: distinguishing morphology and discordant display of Thy 1 and class II MHC. Am. J. Respir. Cell Mol. Biol 1, 65–74, 10.1165/ajrcmb/1.1.65 [PubMed: 2576218]

36. McQualter JL, Brouard N, Williams B, Baird BN, Sims-Lucas S, Yuen K et al. (2009) Endogenous fibroblastic progenitor cells in the adult mouse lung are highly enriched in the sca-1 positive cell fraction. Stem Cells 27, 623–633, 10.1634/stemcells.2008-0866 [PubMed: 19074419]

37. Liu J., Sakurai R. and Rehan VK. (2015) PPAR-gamma agonist rosiglitazone reverses perinatal nicotine exposure-induced asthma in rat offspring. Am. J. Physiol. Lung Cell. Mol. Physiol 308, L788–L796, 10.1152/ajplung.00234.2014 [PubMed: 25659902]

38. Rehan VK, Sakurai R, Wang Y, Santos J, Huynh K and Torday JS (2007) Reversal of nicotine-induced alveolar lipofibroblast-to-myofibroblast transdifferentiation by stimulants of parathyroid hormone-related protein signaling. Lung 185, 151–159, 10.1007/s00408-007-9007-0 [PubMed: 17401602]

39. Garcia O, Carraro G, Navarro S, Bertoncello I, McQualter J, Driscoll B et al. (2012) Cell-based therapies for lung disease. Br. Med. Bull 101, 147–161, 10.1093/bmb/ldr051 [PubMed: 22279079]

40. Han W., Yu Y. and Liu XY. (2006) Local signals in stem cell-based bone marrow regeneration. Cell Res. 16, 189–195, 10.1038/sj.cr.7310026 [PubMed: 16474433]

Clinical perspectives

- The present study investigates the effect of perinatal nicotine exposure on offspring bone marrow mesenchymal stem cell differentiation, which is critical for lung injury repair.
- Using a rodent model, we show that perinatal nicotine exposure enhances bone marrow mesenchymal stem cell differentiation to a myogenic phenotype, which is not conducive for effective lung injury repair; however, concomitant administration of a potent PPARγ agonist blocks this effect, virtually restoring their lipofibroblastic, hence, injury repair potential.
- Our findings are particularly important to understand a potential novel mechanism underlying chronic lung disease susceptibility in developmentally smoke/nicotine exposed individuals and suggest a potentially effective therapeutic approach to block this susceptibility.

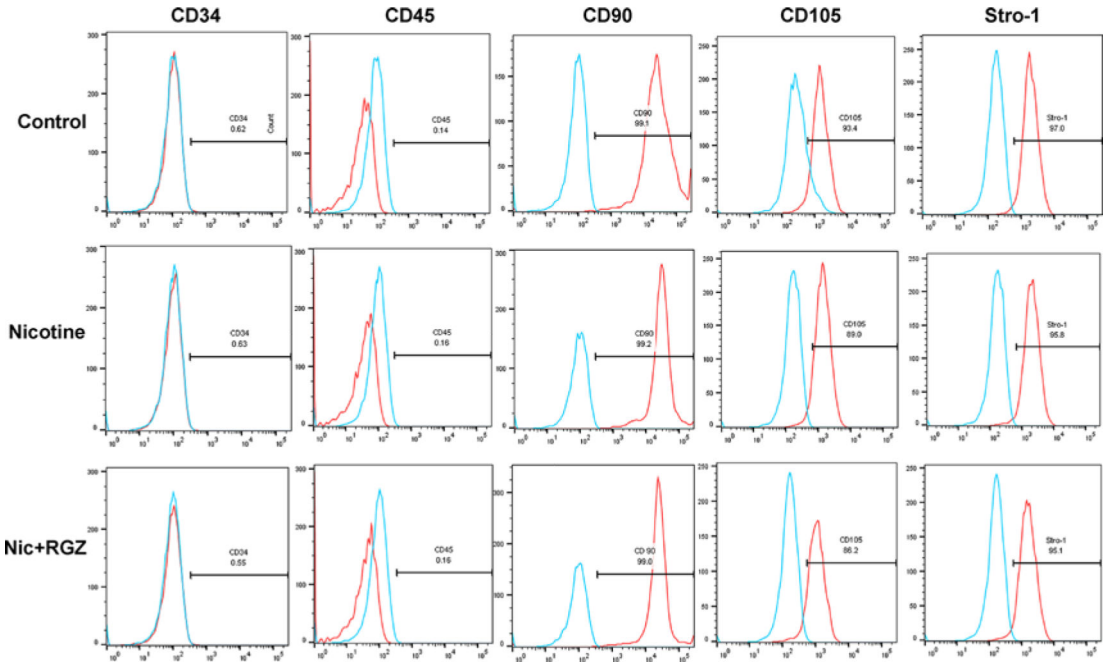

Figure 1. Characterization of bone marrow mesenchymal stem cells

Passage 3 BMSCs isolated from animals from different conditions at postnatal 21 were subjected to fluorescence-activated cell sorting using anti-CD34, anti-CD45, anti-CD90, anti-CD105, and anti-Stro-1 antibodies and analyzed using FlowJo software. Almost all control cells were negative for CD34 and CD45, >90% were positive for CD105, >95% were positive for CD90 and Stro-1. Nicotine and nicotine + rosiglitazone treatments did not affect the percentage of cells expressing these cell surface markers. The multipotent potential of these cells was confirmed by their induction to adipocytes (positive ORO staining), myocytes (positive α-SMA staining), and osteocytes (positive Alizarin red S staining).

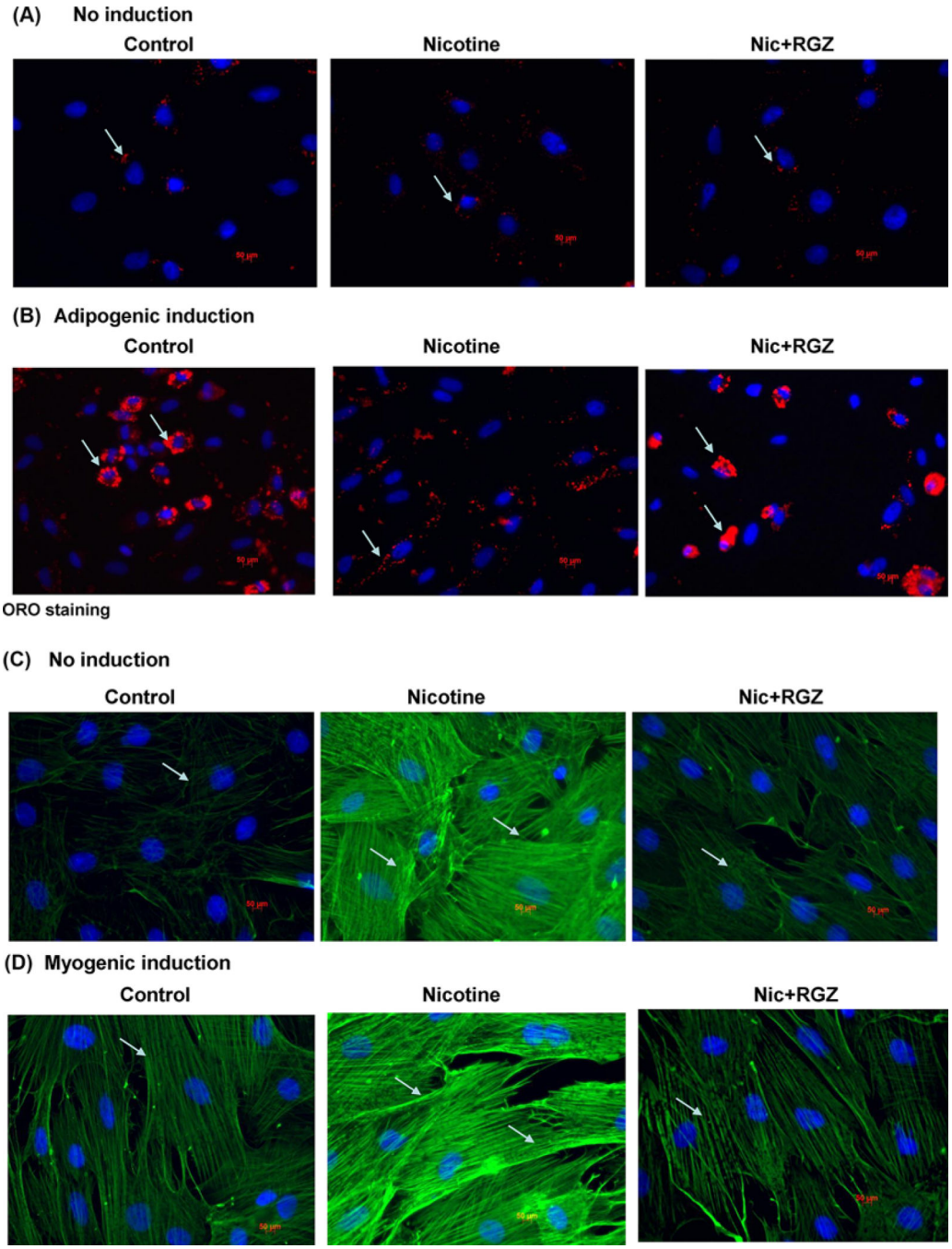

Figure 2. Effect of perinatal nicotine exposure on BMSC adipogenic and myogenic potential

Passage 3 BMSCs isolated from animals from different conditions at postnatal 21 were examined for adipogenic and myogenic differentiation with and without adipogenic and myogenic induction, respectively. The control BMSCs exhibited virtually no ORO staining and very little α-SMA staining at baseline (**A** and **C**), but after adipogenic and myogenic inductions, there were strongly positive ORO and α-SMA staining, respectively (**B** and **D**). Compared with controls, perinatal nicotine (1 mg/kg) exposed cells demonstrated decreased lipid, and increased α-SMA staining, upon adipogenic and myogenic inductions,

respectively (B and D). This effect was blocked by concomitant perinatal treatment with rosiglitazone (RGZ, 3 mg/kg) (B and D) (N=3; representative immunofluorescence images are shown).

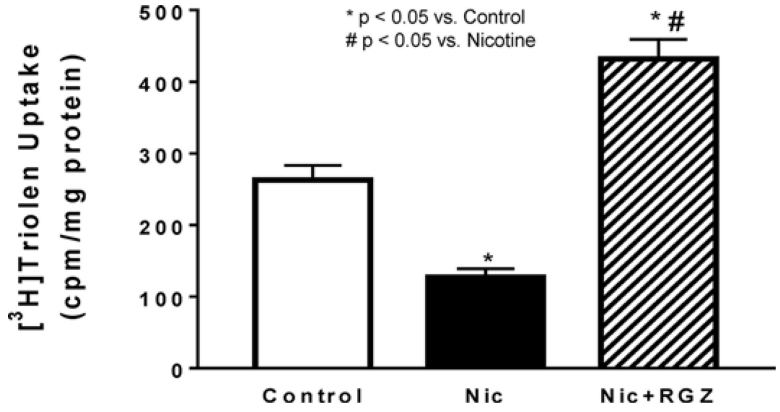

Figure 3. Effect of perinatal nicotine exposure on BMSC adipogenic function, as assessed by [^{3}H]triolein uptake

[^{3}H]triolein uptake was also significantly decreased in perinatal nicotine-exposed BMSCs, an effect that was effectively blocked by simultaneous perinatal rosiglitazone (RGZ) treatment; in fact, RGZ-exposed BMSCs had even higher triolein uptake compared with the untreated controls. N=4; the values are mean ± SEM, $^*P$<0.05, $^{\#}P$<0.05 versus nicotine.

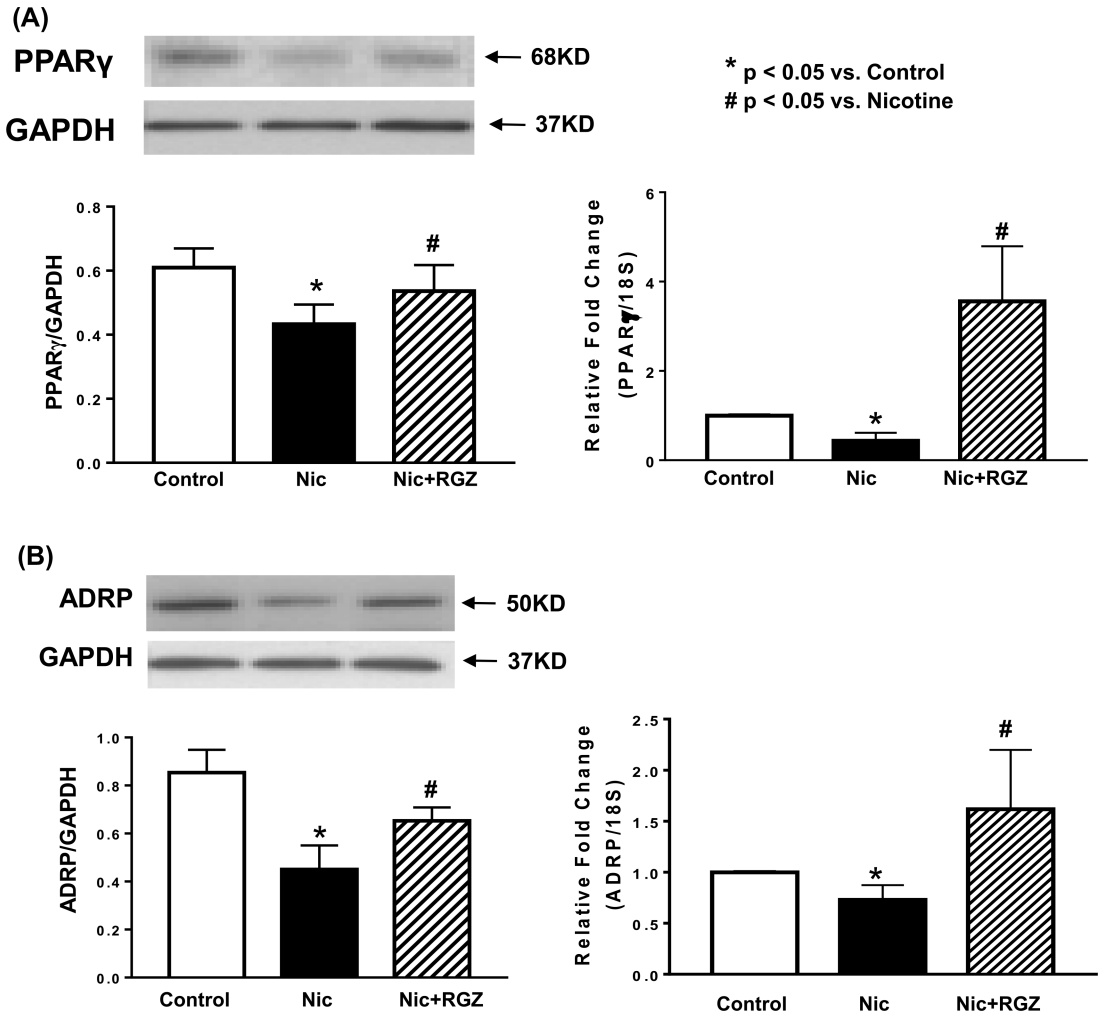

Figure 4. Effect of perinatal nicotine exposure on key lipofibroblast differentiation markers by bone marrow mesenchymal stem cells

PPARγ, a key lipofibroblast differentiation marker, and ADRP, a downstream target of PPARγ, were determined at both protein and mRNA levels. PPARγ expression was inhibited at both protein and mRNA levels and treatment with rosiglitazone (RGZ) blocked this effect (**A**). Similarly, perinatal nicotine exposure down-regulated ADRP expression at both protein and mRNA levels, with partial blockage of this effect with perinatal RGZ treatment (**B**). *N*=4; the values are mean ± SEM, $^{*}P<0.05$, $^{\#}P<0.05$ versus nicotine.

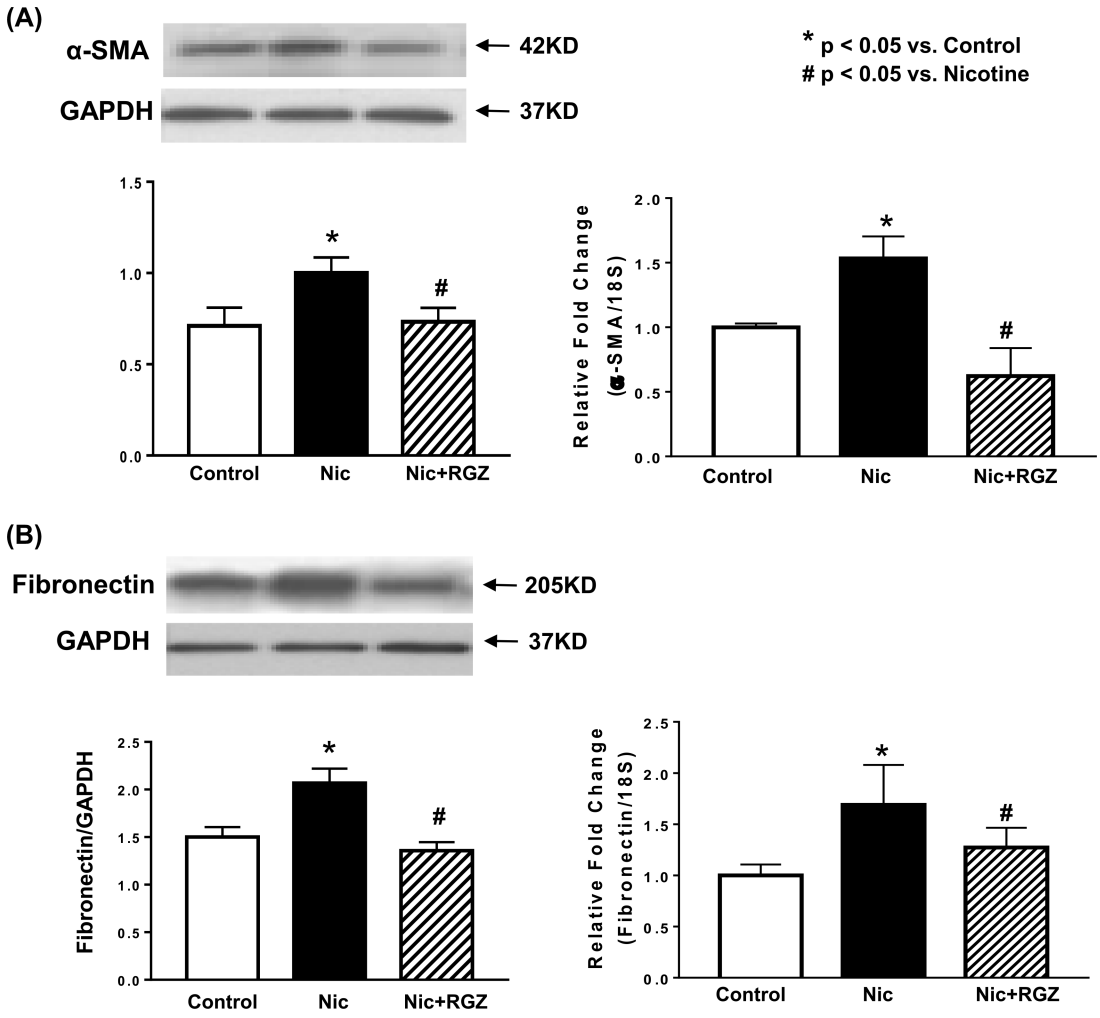

Figure 5. Effect of perinatal nicotine exposure on key myofibroblast differentiation markers by bone marrow mesenchymal stem cells

Myofibroblast differentiation markers α-SMA (**A**) and fibronectin (**B**) were determined at both protein and mRNA levels, both of which were increased with perinatal nicotine exposure, an effect that was blocked by perinatal rosiglitazone (RGZ) treatment (A and B). N= 4; the values are mean ± SEM, $^{*}P<0.05$, $^{\#}P<0.05$ versus nicotine.

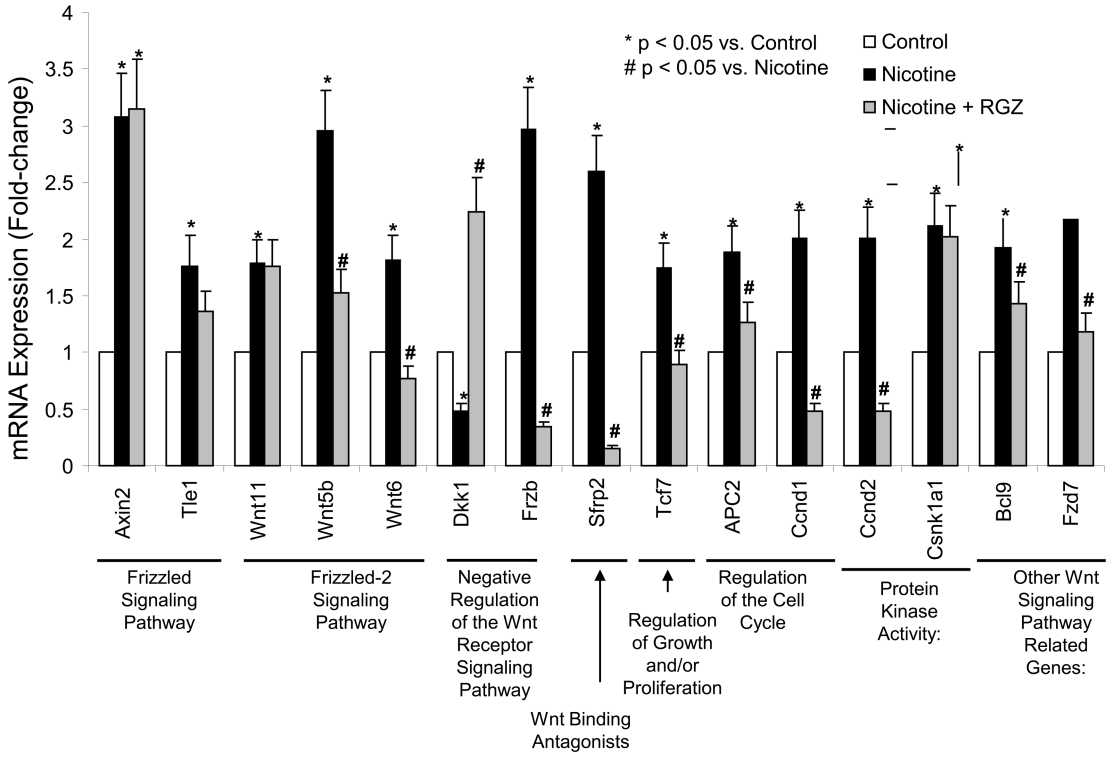

Figure 6. Effect of perinatal nicotine exposure on bone marrow mesenchymal stem cells Wnt signaling

Wnt-specific array (SABiosciences), which probes for 84 specific genes involved in Wnt signaling was performed. In the perinatal nicotine exposed BMSCs, 14 genes showed >2-fold up-regulation, and one gene had >2-fold down-regulation. Ten out of the 14 up-regulated genes, and the only down-regulated gene were normalized in the RGZ- treated group. N=3; the values are mean ± SEM, $^{*}P$<0.05, $^{\#}P$<0.05 versus nicotine.